Available online at www.sciencedirect.com
SCIENCE DIRECT®
International Journal of Heat and Mass Transfer 49 (2006) 2829–2839
International Journal of HEAT and MASS TRANSFER
www.elsevier.com/locate/ijhmt

Effect of nucleation site spacing on the pool boiling characteristics of a structured surface

Nitesh D. Nimkar [a,*], Sushil H. Bhavnani [b], Richard C. Jaeger [c]

[a] *Intel Corporation, 5000 W Chandler Blvd, Mail Stop: CH5-157, Chandler, AZ 85226, Azerbaijan*
[b] *Department of Mechanical Engineering, Auburn University, 201 Ross Hall, Auburn 36849-5341, United States*
[c] *Alabama Microelectronics Science & Technology Center, Auburn University, 200 Broun Hall, Auburn 36849-5341, United States*

Received 23 September 2005; received in revised form 16 February 2006
Available online 27 April 2006

Abstract

Pool boiling characteristics of pyramidal shaped re-entrant cavities (characteristic size 40 μm) etched in silicon were evaluated in this study. A test surface was fabricated to totally eliminate back heat loss and minimize spreading in the substrate. The effect of inter-cavity spacing and convection plumes from a heat source located below the test surface on nucleate boiling parameters is documented. High speed photography was used to record and quantify the bubble departure frequency, the departure diameter, the active site density and to observe the effect of interaction between neighboring nucleation sites. Experiments were conducted in saturated FC 72 at atmospheric pressure.

Keywords: Pool boiling; Re-entrant cavities; Departure diameter; Bubble departure frequency; Active site density; Immersion cooling and thermal management of electronics

1. Introduction

Increases in the number of transistors on microprocessor chips cause an attendant increase in the heat generated in the device. The resulting high heat flux has to be dissipated by increasingly aggressive and innovative methods. Both single-phase and phase-change methods using dielectric liquids are suitable candidates. It is widely recognized that enhancements in surface characteristics can augment phase-change cooling performance. This has led to several recent studies that attempt to provide an understanding of nucleate boiling from enhanced surfaces. The goal is to eventually develop models to accurately predict the various parameters in nucleate boiling so as to design reliable and predictable cooling systems. Research on enhanced surfaces is focused on elimination of overshoot, maximizing critical heat flux (CHF) and on improving the slope of the boiling curve.

Overshoot, for a heat flux controlled experiment, is the sudden drop in the superheat at a constant heat flux caused by the lack of vapor nuclei on the surface, exposing the surface to high superheats. The critical heat flux (CHF), as the name indicates its importance, is the maximum heat flux in the nucleate boiling regime and after which any increase in the heat flux shifts the operating point to the film boiling regime for a heat flux controlled experiment. Increasing the CHF will primarily increase the nucleate boiling regime resulting in efficient thermal management. Lastly the focus is on improving the slope of the boiling curve. A high slope indicates a high heat transfer coefficient.

2. Background

A naturally pitted surface on which nucleation is being observed has random nucleating sites. The study of the existence of interactions between nucleating sites and their

* Corresponding author. Tel.: +48 05528185; fax: +48 05521295.
E-mail address: nitesh.nimkar@intel.com (N.D. Nimkar).

0017-9310/$ - see front matter © 2006 Elsevier Ltd. All rights reserved.
doi:10.1016/j.ijheatmasstransfer.2006.02.018

Nomenclature

d_d	departure diameter
f	bubble departure frequency
q''	heat flux
S/d_d	ratio of the inter-cavity spacing and the departure diameter
ΔT	wall superheat

Greek symbol

v	shape parameter (defined by Chekanov [1])

nature, was initiated by Chekanov [1]. In a study of motion pictures of inter-site interactions Calka and Judd [2] found attractive and repulsive reactions between nucleating sites and these were compared with a dimensionless separation distance S/d_d (spacing between nucleation sites/departure diameter). Recently, Golobič and Gjerkeš [3] developed a technique for activating nucleation sites using laser beams to facilitate direct measurements of interaction between active nucleating sites. They concluded that the interactions resulted in the net decrease in activity of the two sites or the decrease in one with the increase in the other or in the worst case, deactivation of one of the sites.

Research has shown that heat transfer augmentation can be achieved by using structured surfaces or surface enhancements. Micro-pyramidal re-entrant cavities, a type of surface enhancement, arranged in the form of square cavity arrays etched in silicon were used by Bhavnani et al. [4] to simulate a multichip module. Experiments were conducted in FC 72 and the effect of neighboring microelectronic devices was studied. A CHF of 39.4 W/cm^2 was reported for the structured surface. Baldwin et al. [5] conducted a study using bulb shaped re-entrant cavities etched in silicon. Effect of cavity spacings with a center to center distance of 0.5, 1.0 and 1.5 mm and active/inactive neighbors at a power level of 50% of that of the incipient heat flux of the test heater was documented. The simulation of the multichip module was a roman cross, similar to the one used by Bhavnani et al. [4] and experimentation revealed that the increase in the cavity densities resulted in a decrease of the wall superheat. A maximum CHF of 44.3 W/cm^2 was reached for the 1.5 mm spaced surface. You et al. [6] conducted experiments in FC 72 at 35 °C and 1 atmosphere to document the effect of an active and a powered heater below the test heater. When the lower heater was in the boiling stage it showed a strong effect on the boiling incipience of the test heater. Boiling was initiated at a much cooler temperature (less than 15.0 °C). This may have been due to the cavity seeding, on the test heater, caused by the rising bubbles. Baldwin et al. [5] concluded that the bulb shaped re-entrant cavity underperformed where temperature overshoot was concerned in comparison with the pyramidal re-entrant cavity. In a study involving jet impingement of FC 72 on a square thermal chip Chrysler et al. [7] reported that for pool boiling, a maximum heat flux of 45.0 W/cm^2 was obtained at a chip temperature of 85.0 °C corresponding to a 19.0 W chip with out reaching CHF. The researchers attributed this to additional heat dissipation due to natural convection from the substrate surface and by nucleate boiling in the immediate vicinity of the chip. Chang and You [8] documented the boiling heat transfer phenomenon from micro-porous and porous surfaces in saturated FC 72 using five different sized diamond particles. An significant finding was that the CHF varied with the coatings, suggesting that CHF was not only a function of the liquid but also depended on surface properties. The CHF ranged from approximately 15.0 W/cm^2 for the plain surface to a maximum of approximately 28.0 W/cm^2. Kubo et al. [9] studied boiling heat transfer for four surfaces with re-entrant cavities having mouth diameters of 1.6 μm and 3.1. The test section was prepared by bonding a 10 mm × 10 mm silicon chip to a glass substrate. Experimentation was done in FC 72 at two levels of subcooling of 3.0 K and 25.0 K. In the nucleate boiling region the chips with 0.1 mm spacing showed the best heat transfer performance. It was conjectured that the optimal size of cavity was larger than the two sizes studied and CHF values from 15.7 W/cm^2 to 16.2 W/cm^2 were reported. Moghaddam et al. [10] conducted a pool boiling study using copper and graphite foams in FC 72. Experimentation revealed a CHF of approximately 11.0 W/cm^2 for the 30 ppi (pores per inch) copper foam and approximately 12.0 W/cm^2 for the 80 ppi copper foam. The plain surface had a CHF of approximately 10.2 W/cm^2. El-Genk and Parker [11] investigated pool boiling of saturated and subcooled FC-72 on a smooth copper surface and porous graphite. The surface under investigation was placed in a Teflon block filled with translucent epoxy. The heating element was a 0.1 mm diameter Nichrome wire. A CHF of 16.9 W/cm^2 was reported for the smooth copper surface.

2.1. Bubble departure diameters and departure frequency

The vehicle of heat removal in two phase analysis is the bubble and hence the departure diameter and the frequency of departure affect the rate of heat transfer. Bubble nucleation growth and the subsequent mixing within the boundary layer directly impact the bubble departure diameter and frequency.

Various researchers have documented different trends for the effect of heat flux on bubble departure diameters and frequency. The relation between frequency and departure

diameter as documented by McFadden and Grassmann [12], and Ivey [13] showed that with the increase in the departure diameter the bubble emission frequency decreased. In their experimentation on pool boiling in dichloromethane on a horizontal glass substrate coated with stannic oxide, Judd and Hwang [14] visually observed the surface and found that as the heat flux increased the departure radius decreased. The departure frequency showed an increasing trend with heat flux. Nakayama et al. [15] conducted experiments in water, R-11, and liquid nitrogen on a tunneled surface. They documented an increase in departure frequency and a decrease in the departure diameter with the increase in heat flux. Fournelle et al. [16] performed an optical study for enhanced heat transfer from a heat sink for microelectronic cooling applications. The bubble departure diameter increased from 0.225 mm to 0.34 mm with the increase in heat flux. The frequency of departure showed a reducing trend with the increase in the heat flux. In a further development from this research, Bhavnani et al. [17] found that the contribution of latent heat as a heat dissipation mechanism was less than 16% and that boundary layer mixing had a greater impact on the bubble departure diameters.

In a visualization study Pascual et al. [18] found that the average frequency increased and then decreased with the increase in heat flux. A negligible effect of increasing heat flux on bubble diameter was documented by Rini et al. [19] for experimentation in FC 72 on synthetic diamond plate with Ni–Cr serpentine heaters. Ramaswamy et al. [20] documented an increase in bubble departure diameter with the increase in wall superheat for pool boiling in FC 72 from micro-channels. The bubble departure frequency initially increased and then decreased with the increase in wall superheat. It was hypothesized that this behavior of frequency was due to the small pool size and that frequency would show an increasing trend with the increase in wall superheat for a larger pool size. Recently, Zhang and Shoji [21] conducted experiments in distilled water to study bubble interactions between two cylindrical cavities etched in silicon and the spacing between them was varied. An interesting find was that for a S/d_d ratio of 1.5 bubble departure diameter and frequency showed an increasing trend with increase in heat flux. Between a S/d_d ratio of 1.5 and 2.0 the frequency increased and then dropped to a S/d_d of 3.0 where the frequency was the same as on an isolated site.

It is obvious that nucleate boiling from structured surfaces is a very complex phenomenon. Primary factors affecting heat transport appear to be cavity geometry, spacing, substrate thermal conductivity and fluid properties. Matters are further complicated when surface structures are not homogeneous.

3. Experimental setup

The present study was aimed at collecting pool boiling data with minimal losses (back heat loss and heat spreading in the substrate also known as substrate spreading) for a vertically oriented test surface with pyramidal micro-re-entrant cavities etched in silicon. Spreading was minimized by using glass, a low conductivity substrate. The heat source, a serpentine aluminum heater (6900 μm wide), was sandwiched between two glass wafers to eliminate the back heat loss as seen in Fig. 1a. Identical and equally spaced micro-pyramidal cavities with a 240 μm square base and a 40 μm square mouth, as seen in Fig. 1b, were fabricated in ⟨1 0 0⟩ silicon using anisotropic etching. The cavity spacings with center-to-center spacing of 0.5 mm (225 cavities), 0.75 mm (100 cavities) and 1.0 mm (64 cavities) were fabricated in addition to a plain surface and these surfaces will be referred to throughout the paper as surface 1, surface 2, surface 3, and the plain surface, respectively. To study the effect of convective plumes from a neighboring heat source located below the test heater, two different heater spacings were used. A spacing equal to the width of a single heater and the other equal to twice that were fabricated. The fabricated cavity arrays were anodically bonded to glass to eliminate spreading effects. Fabrication details can be found in Nimkar et al. [22]. A crude FEA analysis was done using ANSYS and the numerical results showed only 4.0% heat loss from the unbonded glass surface at CHF.

Experimentation was done in FC 72 at atmospheric pressure. The experimental setup, as seen in Fig. 2, consisted of an outer deionized water tank and an inner FC 72 tank. The inner tank housed the test surface on a copper support. FC 72 was indirectly heated to its saturation temperature by heating the deionized water in the outer tank using a circulation resistance heater. The hot FC 72 vapor was cooled in a water cooled helical condenser coils, with one end open to atmosphere. A calibrated k-type thermocouple monitored the fluid temperature. Heater/temperature sensors were calibrated using a thermistor. The calibration was done by immersing the specimen along with the thermistor in a constant temperature bath and the effect of temperature on the heater/temperature sensors was plot and used for wall temperature calculations. Additional details on calibration are outlined in Nimkar [23] sandwiching the heater in between two glass wafers resulted in one dimensional heat transfer data. This enabled the use of simple one dimension resistance network analogy to compute the surface temperature.

Repeatability in data collection was ascertained before starting data collection. Data from six consecutive runs showed great repeatability where data from a run matched that from an earlier run.

Prior to the start of a run FC 72 was completely degassed and the gas content was monitored using a Seaton–Wilson Aire-ometer. The first run, designated as the "No Previous Nucleation History" (NPNH) run and was started after overnight cooling of the fluids. The heat flux in W/cm^2 was obtained by dividing the product of the voltage drop across the heater and current, supplied using a DC power supply, by the array area (silicon area). Array area was selected due to minimal spreading achieved by the use of a very low conductivity substrate. The superheat

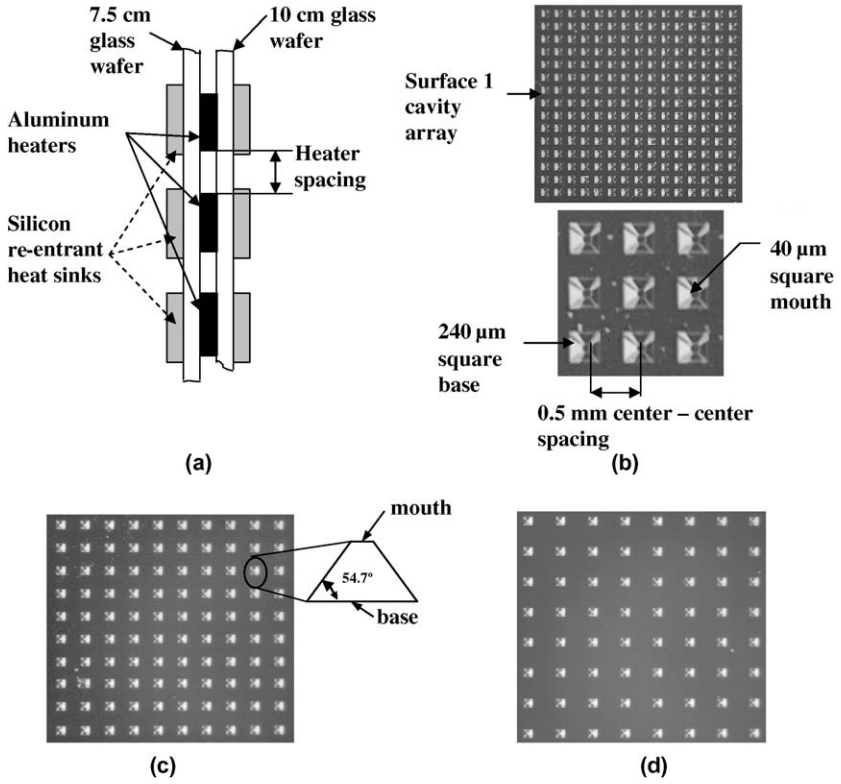

Fig. 1. (a) Symmetric arrangement on a glass substrate (not to scale); (b) surface 1 and surface 1 details showing cavity characteristics, and inter-cavity spacing; (c) surface 2—0.75 mm inter-cavity spacing with a 2D schematic of the pyramidal cavity; (d) surface 3—1.0 mm inter-cavity spacing.

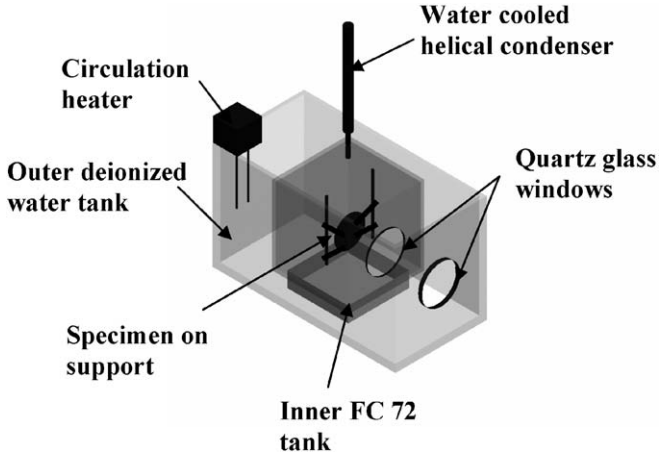

Fig. 2. Schematic of the experimental setup.

was calculated by a simple one dimensional conduction analysis through the glass and silicon. Current was increased till the superheat dramatically increased which indicated CHF. Current was then lowered in small steps to zero current. "The previous nucleation history" (PNH) run was initiated after the NPNH run following the same procedure as above. The same procedure was followed on the next day to ascertain repeatability of the data, but this time the big jump in the superheat did not occur, validating the vapor-trapping ability of the re-entrant cavity shape. The uncertainty in heat flux was calculated to be ±0.8%. Data from all experiments showed excellent repeatability.

A Kodak Motioncorder® was used to capture motion at 400 frames per second (fps) on nucleation. The illumination was done using two halogen lamps place on the front side of the quartz glass. The bubble departure diameter was measured on the screen at three different locations at the same heat flux. The average of the measurements was then converted using a magnification factor found using a length scale. Similarly, the bubble departure frequency was measured at the same heat flux at three different sites for 100 frames. The average frequency was then multiplied by four (400 fps/100 frames = 4 per second) to yield the actual bubble departure frequency). The bubble departure diameter and the bubble departure frequency were measured with an uncertainty of 3.8% and 2 Hz, respectively. The uncertainty for surface temperature measurement was ±10%. All the uncertainties in the present work were calculated using the procedure outlined by Kline and McKlintock [24].

4. Results and discussion

The present paper examines the effect of inter-cavity spacing and convective plumes from a heat source located below the test heater on the nucleate boiling performance, bubble nucleation parameters, active site density, and CHF for a vertically oriented test surface with micro-pyramidal cavities immersed in saturated FC 72.

4.1. Effect of cavity spacing

Nucleate boiling performance and bubble nucleation parameters were studied for three different cavity spacings in addition to a plain surface. An important finding during analysis was that the temperature of the sandwiched serpentine heater was not equal to the surface temperature much contrary to research in high conductivity silicon substrate by Bhavnani et al. [4], Baldwin et al. [5] and Fournelle et al. [16]. This temperature difference between the heater and surface temperatures, due to the high thermal resistance of glass, was a function of heat flux.

Though the specimen was designed for symmetry, both the surfaces did not nucleate at the same time for all the test surfaces except surface 1. Detailed analysis showed that the lack of symmetry was due to small differences in the thickness of the glass wafers due to manufacturing tolerance. Once nucleation was initiated on one surface then most of the heat dissipated through that surface, drastically reducing the heater temperature. This prevented the other surface from nucleating at the same time and kept it in the natural convection region. The surface in natural convection would nucleate later at a higher wall superheat after which symmetric conditions would be restored till CHF and for the decreasing part of the NPNH run. For the PNH run, the cavities that were active on both sides before the end of the NPNH run nucleated when power was supplied, ensuring symmetric conditions for the PNH run. The logic, that perfect symmetry is not achieved because of the difference in the thickness of the glass wafers, was confirmed when for all the test sections the nucleating surface for the NPNH run always nucleated first for every NPNH run for that test surface. In light of this all the data analysis was performed on decreasing heat flux part of the cycle.

For the NPNH runs at incipience all the sites on all the structured surfaces nucleated simultaneously, indicating that the spreading was minimized. This pattern was not observed by Bhavnani et al. [4] and Baldwin et al. [5] who used a high conductivity silicon as a substrate. Fig. 3 is a still image showing 100% nucleation at onset of nucleate boiling for surface 1 (0.5 mm spacing).

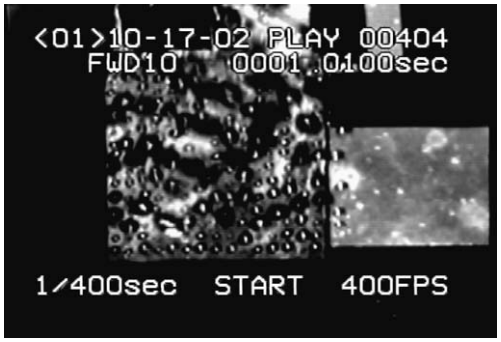

Fig. 3. Still image showing 100% nucleation at ONB for surface 1.

During experimentation the heat flux was increased till CHF and then reduced to zero power for both NPNH and PNH runs. As mentioned earlier at the onset of nucleate boiling for the NPNH run, the entire surface was active and stayed active till CHF. The pool boiling curves for the decreasing part of the heat flux and for the NPNH runs are shown in Fig. 4. The nucleate boiling performance was evaluated by comparing the pool boiling curves for the structured surfaces with the pool boiling curve for the plain surface. Fig. 4 shows the comparison. An enhancement is achieved when a surface can dissipate more heat at the same surface temperature or can reduce the surface temperature at the same heat flux. The constant heat flux analysis line in Fig. 4 was used to evaluate the wall superheat performance of the surfaces. A heat flux of 7.8 W/cm^2, a value mid way in the nucleate boiling region, was selected for the analysis. At a heat flux of 7.8 W/cm^2, the plain surface had a wall superheat of 31 °C where as surface 2 (0.75 mm spacing) was the coolest with a wall superheat of 24 °C. While surface 3 (1.0 mm spacing) achieved a wall superheat of 26 °C, the most densely packed surface 1 (0.5 mm spacing) underperformed, compared to the plain surface, with a wall superheat of 33 °C. For the constant wall superheat analysis a wall superheat of 24 °C was selected since this yielded a surface temperature of 80 °C which is relevant to microelectronics cooling. Analyzing a constant wall superheat line in Fig. 4, surface 2 and surface 3 had a heat flux dissipation of 7.8 W/cm^2 and 6.6 W/cm^2, respectively when the plain surface was dissipating 4.7 W/cm^2 and surface 1 (0.5 mm spacing) was dissipating the least heat flux of 2.2 W/cm^2 at that wall superheat.

A PNH run immediately followed the NPNH run. The reason for conducting a PNH run was to check the vapor trapping ability of the re-entrant pyramidal cavities. At the last data points before power switch off, for the NPNH runs, the cavities which were active went into a sporadic nucleation mode, i.e., cavities were randomly nucleating at different frequencies from different locations. At the start of the PNH run, the cavities which were in the sporadic nucleation mode became active unlike that seen for the NPNH runs. With the increase in the heat flux the size of the departing bubbles increased (the effect of heat flux on departure diameters is mentioned later in this section). With the further increase in heat flux more sites on the surface activated and this continued until the entire surface was nucleating. This point was approximately achieved at a heat flux approximately equal to 40% of CHF. From this point on there is no difference between the PNH and NPNH runs.

Owing to the early nucleation, i.e., nucleation at very low heat fluxes, there were minimal overshoots (maximum overshoot of 1.5 °C) compared to the NPNH run. Except for the above mentioned difference the PNH runs for the isolated surfaces were similar to the NPNH runs for the isolated surfaces. Similar behavior in overshoots was reported by Bhavnani et al. [4] and Baldwin et al. [5].

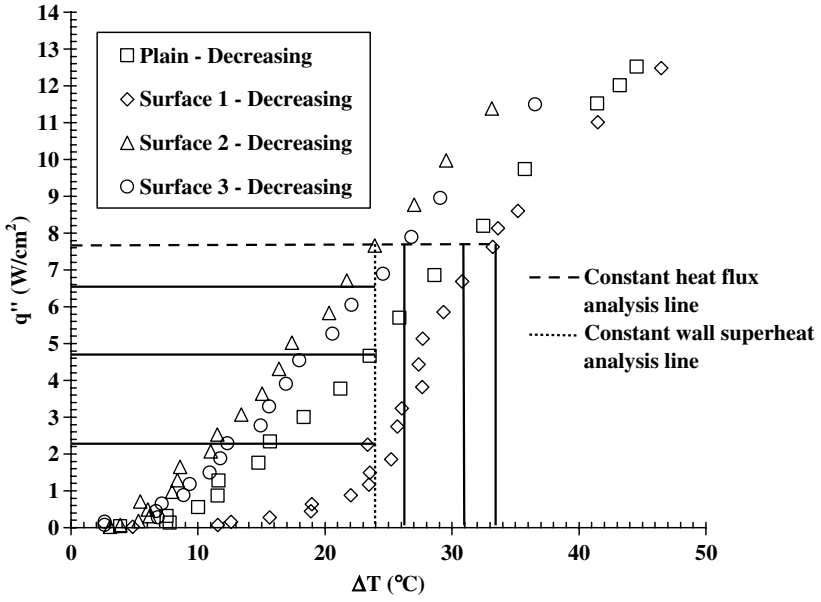

Fig. 4. Pool boiling curves for the decreasing heat flux part of the experiment and for the NPNH runs for all surfaces.

The comparison of the performance of the surfaces for the PNH runs was done similar to comparison technique used to analyze performance for the NPNH runs. For the PNH runs, surface 2 showed the best performance by dissipating 7.3 W/cm^2 for the constant wall superheat analysis (at 24 °C) and for the constant heat flux analysis (at 7.8 W/cm^2) had a wall superheat of 25 °C. Surface 1 underperformed by dissipating only 3.6 W/cm^2 for the constant wall superheat analysis (at 24 °C) and for the constant heat flux analysis (at 7.8 W/cm^2) had a wall superheat of 33 °C. Surface 3 and the plain surface had similar performances as seen earlier. The reason for the underperformance of surface 1 (0.5 mm spacing), compared to the plain surface, is addressed below.

A high active site density was expected for the three surfaces since nearly all the heat generated was being dissipated via nucleate boiling. On examining the high speed photography clips for the different surfaces it was found that the active site density (ASD) was greatly affected by the cavity spacing (refer to Fig. 5). The active site density presented in Fig. 5 represents the percent of number of sites active to the total number of cavities in the array. Using the high speed recordings at a particular heat flux, the number of active sites on a structured surface were measured three times and the mean is documented as the ASD. ASD was measured for the decreasing part of the NPNH and LHP–NPNH runs only since the PNH and NPNH runs were similar for that part as discussed earlier.

Fig. 5 plots the ASD as a function of heat flux. It is a well established fact that the ASD decreases with the decrease in heat flux and the same is observed here. Surface 2 (0.75 mm inter-cavity spacing) had the highest ASD. For a NPNH run surface 2 was nearly 100% active where as under the influence of a convective plume (will be explained

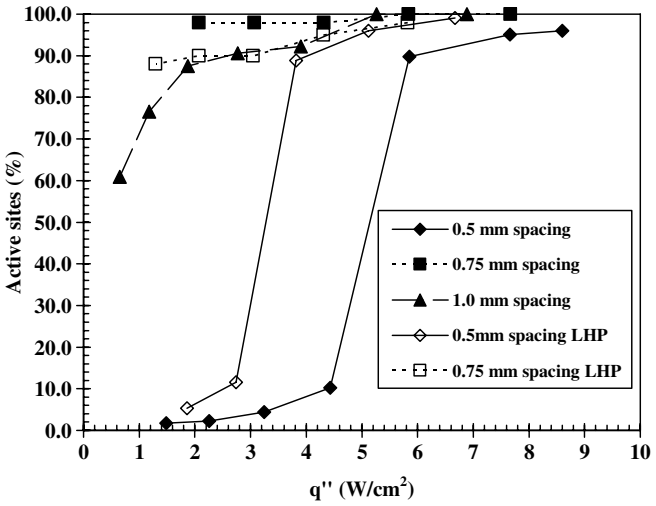

Fig. 5. Active site density as a function of heat flux for different runs.

in the next section) was 89% active for the NPNH run. Surface 1 had the least ASD of all these surfaces for the NPNH runs. A snap-shot view of the nucleation activity for the different surfaces and runs is shown in Fig. 6. The pictures represent the pictorial representation of the ASD for different surfaces and for different runs. The aim is to compare the active site density at low (approximately 0.8 W/cm^2) and a moderate heat flux (approximately 4.0 W/cm^2). These values of heat fluxes were chosen to highlight the ASD performance of the surfaces and runs. It is evident from Fig. 6(a), (c), and (e) that surface 2 was the most active at a very low heat flux. At the moderate heat flux much of surface 1 is inactive where as surface 2 and surface 3 have similar performances. Comparison of Fig. 6(d) and (f) shows that there is no difference between a PHN and NPNH run when the two are compared at

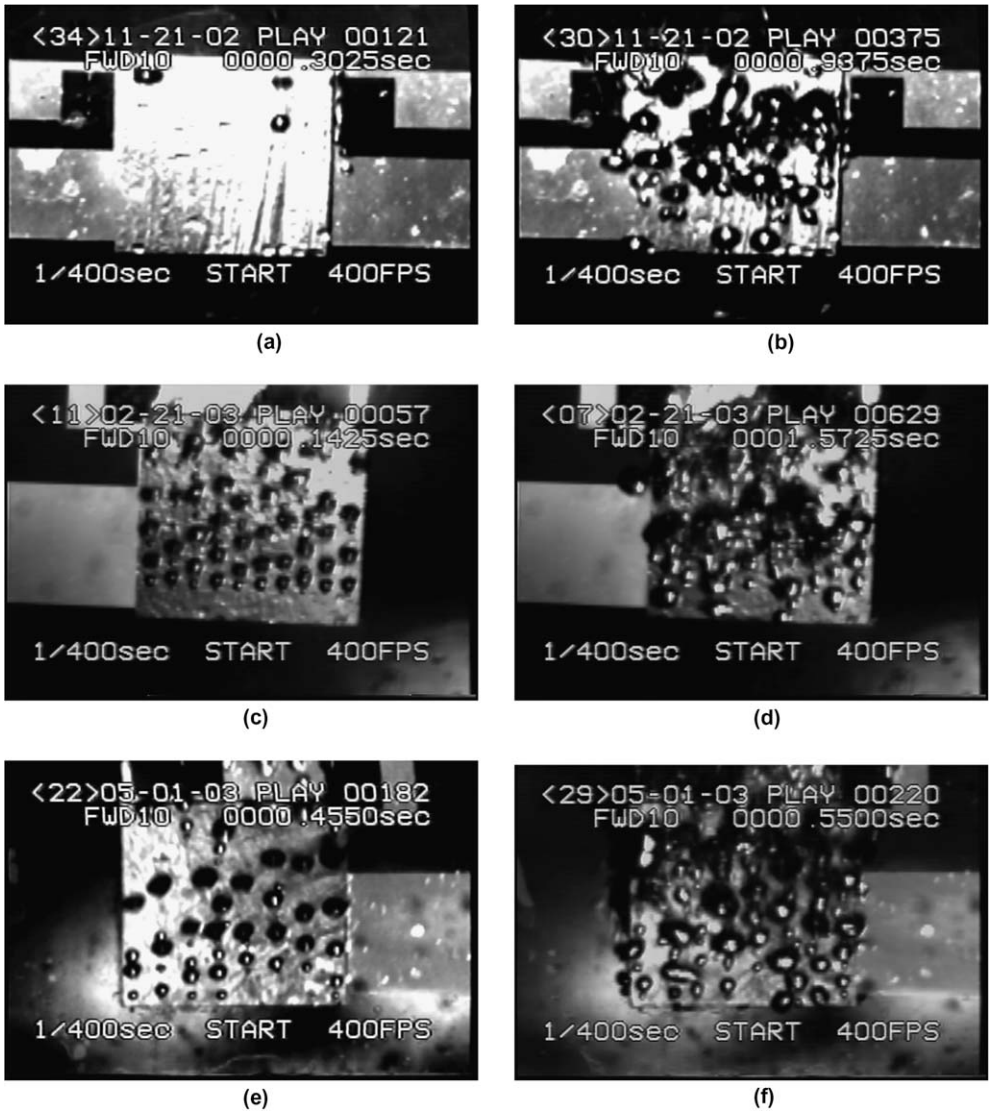

Fig. 6. Surface nucleation snap-shots for different surfaces and runs showing variation in ASD: (a) surface 1—NPNH—0.87 W/cm^2; (b) surface 1—NPNH—4.43 W/cm^2; (c) surface 2—LHP NPNH—0.72 W/cm^2; (d) surface 2—LHP NPNH—4.31 W/cm^2; (e) surface 3— PNH—0.89 W/cm^2; (f) surface 3—PNH—3.89 W/cm^2.

the decreasing part of the heat flux. All the data reported for the present work was collected for the decreasing part of the heat flux.

Preliminary visual observations showed that with the increase in heat flux both the departure diameter and frequency increased. The departure diameter data was collected on NPNH runs only. Diameters were measured on the decreasing heat flux part of the experiment to ensure measurements in a symmetric condition and also because the boiling was intense during the increase in heat flux which made measurement difficult. Fig. 7 shows the effect of heat flux on bubble departure diameter. The departure diameter increased with heat flux for all surfaces. Cavity spacing had little effect on departure diameters. Similar trends in departure diameter were observed by Fournelle et al. [16] for experiments in FC 72. Pascual et al. [18] reported an increase and then a decrease in the departure diameters from experimentation in R-123. Recently, Ramaswamy et al. [20] documented an increase in departure diameter for data collected on micro-porous structures in FC 72. This trend is supported by the data documented by Zhang and Shoji [21] up to a S/d_d ratio of 1.5 and between 2.5 and 3.0. The bubble size was found to be independent of the pore pitch. A contradictory trend, i.e., a decrease in the bubble departure diameter with increase in heat flux was reported by Golobič and Gjerkeš [3] and by Nakayama et al. [15] for experimentation on tunneled surfaces.

In an attempt to understand the reason for the underperformance of surface 1, S/d_d values were calculated examined in light of the findings of Chekanov [1] and Calka and Judd [2] (refer to Fig. 8). For surface 1, surface 2 and surface 3 the S/d_d values ranged from 1.05 to 1.88, 1.70 to 2.50 and 2.17 to 4.22, respectively. Chekanov [1]

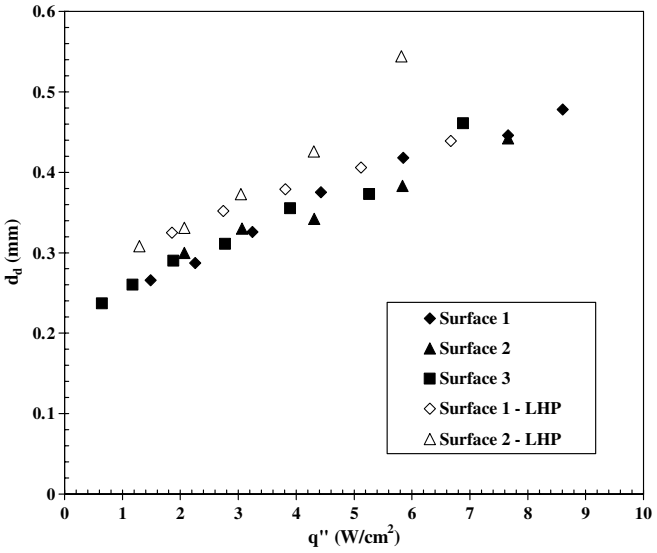

Fig. 7. Comparison of variation of departure diameter with heat flux for all cases.

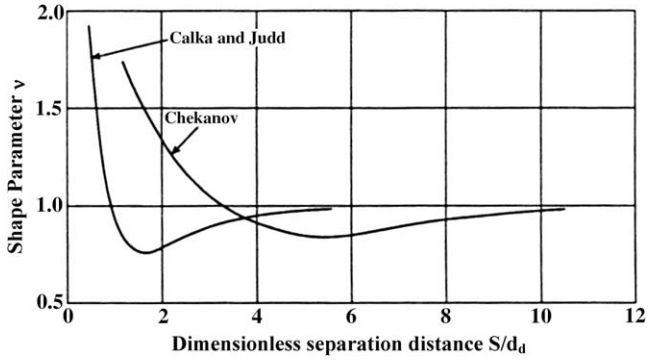

Fig. 8. Comparison of the results of Chekanov [1] and Calka and Judd [2].

found repulsive interaction for S/d_d values less than 3 (where the y-axis variable v was greater than 1) whereas Calka and Judd [2] reported similar interaction for $1 < S/d_d < 3$ and $0 < v < 1$. For the present study the S/d_d values for surface 1 lie deep in the repulsive interaction zone compared to the S/d_d values for surface 2 and surface 3. This implied that there were strong repulsive interactions between nucleating sites on surface 1 than the interactions between nucleating sites on surface 2 and surface 3 resulting in poor performance. Bhavnani et al. [17] reported that latent heat contribution to heat transfer was less than 16% of the total heat dissipated. This indicates that though the cavity density on the densely packed surface 1 was the highest it need not be the coolest surface. Their research showed that boundary layer mixing would greatly affect heat transfer. In the case of surface 1 (0.5 mm spacing) the high nucleation density would have inhibited the boundary layer mixing where the closely packed bubbles would have obstructed the flow of cooler fluid to the surface resulting in elevated temperatures at any given heat flux.

In addition to this surface 2 had the highest ASD for the both the runs. The existence of this indicates that there were favorable interactions between nucleating sites on that surface. The present data collected is not sufficient enough to strongly prove the assertion, but it definitely suggests that there is an optimum inter-cavity spacing, in the neighborhood of 0.75 mm, which will yield the best results for immersion cooled electronics using an enhanced surface similar to that used in this study.

Similar to the effect of heat flux on bubble departure diameters, frequency increased with the increase in heat flux as seen in Fig. 9a for all cases studied. Under the effect of a convective plume from a lower heater the frequency increased compared to the frequency on isolated surface runs. This increase could be due to the sweeping action of the superheated liquid layer moving on the surface of the test heater. A similar trend for the frequency was reported by Ramaswamy et al. [20] (frequency was compared with the wall superheat which can be converted to heat flux using the pool boiling curves). But, at intermediate wall superheats the frequency reduced, this reduction in frequency was attributed to the small pool size (refer to Fig. 9b. It was hypothesized that the frequency would show an increasing trend for a larger pool. Nakayama et al. [15] from experiments in R-11, reported an increase in frequency with the increase in heat flux. Fournelle et al. [16] reported a decreasing trend for the frequency for experimentation in FC 72 but those tests were conducted on a high conductivity substrate unlike the present study.

Another pool boiling parameter focused on was the CHF. CHF is an important parameter since it puts limitations on the application of immersion cooling as a successful thermal management solution because if CHF is reached during cooling it could result in device burn outs. In the present study the average critical heat flux was 12.7 W/cm^2, a number lower than the CHF of approximately 15.0 W/cm^2 predicted by the Zuber correlation

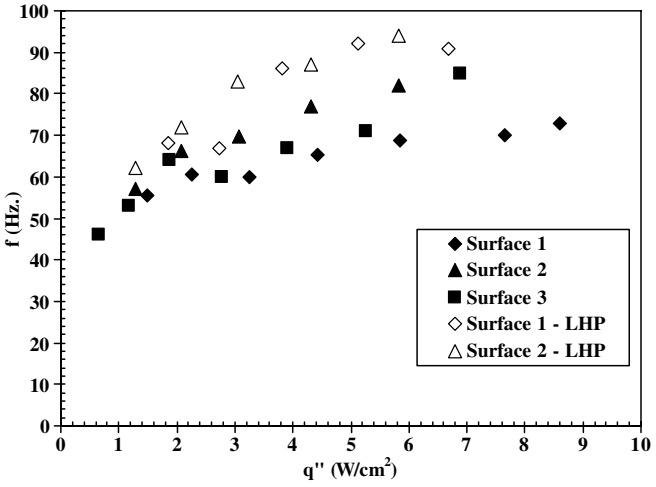

Fig. 9a. Comparison of the effect of heat flux on bubble departure frequency for all cases.

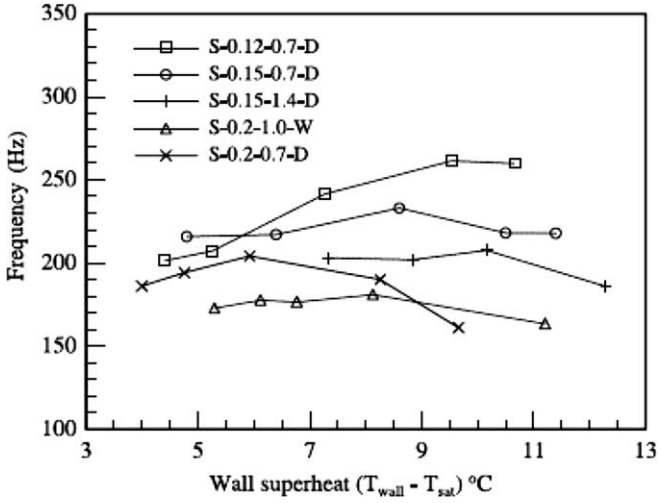

Fig. 9b. Variation of average frequency with wall superheat [20].

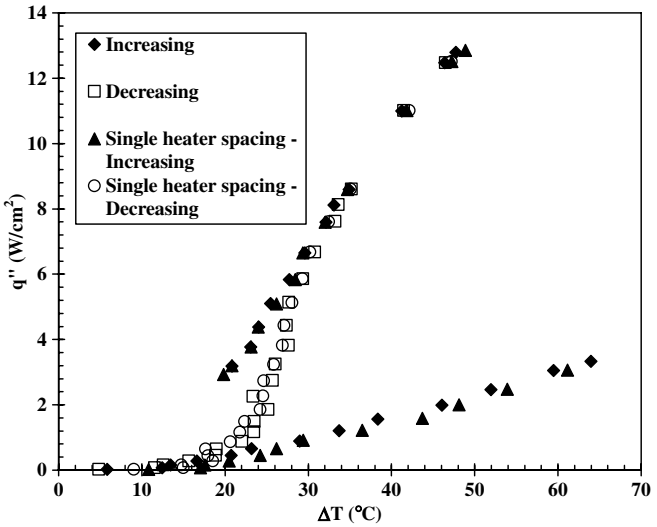

Fig. 10. Comparison of pool boiling curve for surface 1 with the lower heater powered for a heat source at single heater spacing, with the pool boiling curve for an isolated surface 1, NPNH run.

and much less than the CHF for small flat heaters of approximately 21.0 W/cm^2. The Zuber correlation was based on the hydrodynamic instability model for fluids such as water. Analysis showed that the most critical Raleigh–Taylor wavelength for water was 12.2 times higher than that for FC 72. Various researchers have predicted the CHF values to be greater than 21.0 W/cm^2 since high conductivity substrates such as silicon, used by Bhavnani et al. [4] and Baldwin et al. [5], had high substrate spreading effects. Moghaddam et al. [10] reported a CHF of approximately 12.0 W/cm^2 for pool boiling on copper foam structures in FC 72. El-Genk and Parker [11] reported a CHF of 16.9 W/cm^2, a value lower than that predicted by the Zuber correlation. Though not documented in their work, the epoxy used to fill the square cavity in the Teflon block would have reduced heat losses due to spreading and the back heat loss. Kubo et al. [9] reported a heat flux of 15.7 W/cm^2 for experimentation in FC 72 with 3 °C subcooling. The test surface used was designed similar to that used in this study but had a different enhanced surface. In the current work by minimizing spreading effects and eliminating the back heat loss, the CHF reported is less than the values predicted by the traditionally used CHF correlations. In light of the current findings it clear that further research aimed towards the formulation of new CHF correlations for highly wetting fluids would aid the electronics cooling community.

4.2. Effect of convective plumes on nucleate boiling

In the present paper the effect of the lower heater powered to 50% of the incipient heat flux is also documented. These runs were known as "lower heater powered" runs and will be referred to as the LHP runs. The effect of the lower powered heater was seen for two different heater spacings. Heater spacing one corresponded to a spacing equal to the width of the serpentine heater and spacing two corresponded to twice the width of the heater. Instead of showing individual plots for the LHP–NPNH runs, a plot for a LHP run for a particular surface is compared with a plot for an isolated run for the same surface. Refer to Fig. 5 to see the effect of heat flux on ASD for the LHP runs.

Fig. 10 compares the NPNH–LHP single heater spacing run for surface 1 with a NPNH for an isolated surface 1 experiment. The LHP run was similar to the isolated surface run except that the surface was hotter at the start of the experiment by 5 °C. Similar observations were made by Baldwin et al. [5] who reported negligible effect of convective plumes on the nucleate boiling region of the test heater but found that the superheats were higher in the natural convection region compared to those for the isolated surface runs. A similar curve was achieved for the LHP–NPNH single heater spacing run for surface 2 and hence is not shown. For the plain surface the effect of convective plumes was studied for both the heater spacings. Comparison of the curves shows no effect of heater spacing on the pool boiling curves in the nucleate boiling region. As expected, it does affect the natural convection region compared to the pool boiling curves for isolated plain surface runs. As seen in Fig. 10 the pool boiling curves has the classic 'S' shaped appearance due to minimal spreading and elimination of back heat loss. In a similar study LHP–PNH runs were performed and compared with the runs for isolated surfaces (Fig. 11). The LHP runs had similar behavior as the isolated surface PNH runs. A characteristic of the PNH runs was that for all surfaces the runs had nearly no overshoots. A maximum overshoot of 1.5 °C was recorded for the PNH runs. The nucleate boiling performance for the LHP runs was compared using the same technique used to compare the performance of isolated surface. The comparison had results similar to those for the isolated surface runs where surface 2 (0.75 mm spacing)

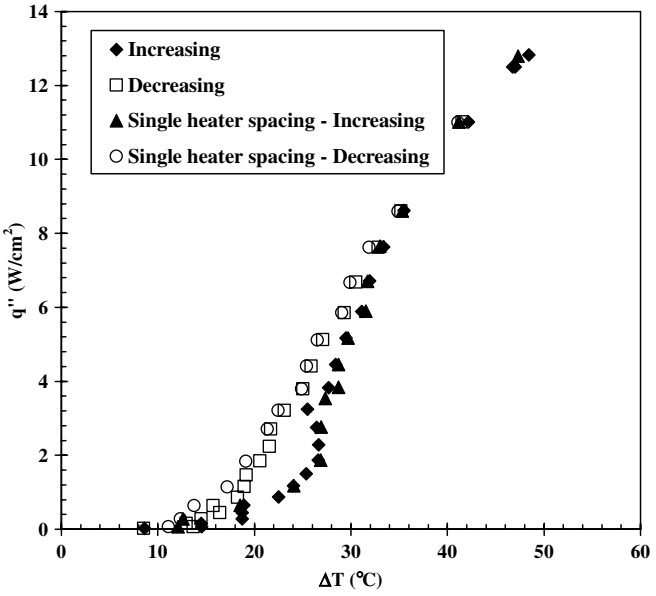

Fig. 11. Comparison of pool boiling curve for surface 1 with the lower heater powered for a heat source at single heater spacing, with the pool boiling curve for an isolated surface 1, PNH run.

was the best performing surface and surface 1 (0.5 mm spacing) underperformed compared to the plain surface.

For all runs the pool boiling parameters lacked specific trends except that the structured surfaces had higher overshoots than the plain surface for the NPNH runs. For the PNH runs minimal overshoots were observed. This pattern in overshoots was documented by Baldwin et al. [5] for experimentation in FC 72 on bulb shaped cavities.

The bubble departure diameters and bubble departure frequency increased under the influence of the convective plumes relative to the values at the same heat flux for isolated surface runs (refer to Figs. 5 and 7). The increase could have been caused due to the improved boundary layer mixing caused by the convective plumes and was found to be a function of cavity spacing. The increase in departure diameters for LHP runs, relative to the departure diameters for isolated surfaces, was more for surface 2 (0.75 mm spacing) than surface 1 (0.5 mm spacing) since for surface 2 more room was available for bubble growth.

5. Conclusions

One dimensional heat transfer data was collected for a vertically oriented test surface with micro-pyramidal re-entrant cavities. Minimal heat losses ensured that all the applied heat was dissipated via phase-change immersion cooling. The use of a low conductivity substrate minimized spreading and led to simultaneous nucleation from all the equally spaced and identically sized cavities on the enhanced heat sink for the NPNH run.

The boiling curves for the structured surfaces were compared with the boiling curve for the plain surface using two types of analyses for all runs. The comparison showed that surface 1 (0.5 mm spacing) with the highest nucleation density underperformed, compared to the plain surface, due to repulsive interactions between nucleating cavities and also due to hindered boundary layer mixing. Surface 2 (0.75 mm spacing) showed the highest heat transfer augmentation. Bubble departure diameter and frequency increased with the increase in heat flux. No effect of cavity spacing was seen on departure diameter and frequency.

The active site density decreased with the decrease in heat flux and was strongly affected by the cavity spacing. Surface 2 had the highest ASD compared to the other surfaces whereas the most densely packed surface, surface 1, had the least ASD. The present data collected definitely suggests that there is an optimum inter-cavity spacing, in the neighborhood of 0.75 mm for which most of the surface remains active for a wide range of heat fluxes. Enhanced surfaces with similar geometric characteristics will yield the best results for immersion cooled electronics.

A multichip module was simulated to study the effect of convection plumes off a neighboring heat source, powered at 50% of its nucleation heat flux, located below the test heater. Pool boiling analysis for two different heater spacings revealed that the lower powered heater only affected the natural convection region when compared to an isolated run for the same surface. The superheated liquid on the test heater due to a powered lower heater influenced the departure diameter and frequency by increasing them compared to the values for isolated surfaces. The increase in departure diameters under the effect of a convective plume was found to be a function of cavity spacing which governed the space available for growth and this could have been due to increased boundary layer mixing.

An important finding was that the average CHF achieved (12.7 W/cm^2) was a lower than that predicted by Zuber correlation (15.0 W/cm^2) and a correction for small heaters which estimated it to be 21.0 W/cm^2. It is also important to note that the proposed CHF correlations were developed for water, a highly non wetting liquid compared to FC 72 a highly wetting fluid. Calculations showed that the most dangerous instability wavelength for water was 12.2 times greater than that for FC 72.

Acknowledgements

The test fluid used in this study was provided by the 3M Corporation. Financial support was provided by the Alabama Microelectronics Science and Technology Center.

References

[1] V.V. Chekanov, Interaction of centers in nucleate boiling Translated from, Teplofizika Vysokikh Temperatur 15 (1) (1977) 121–128.
[2] A. Calka, R.L. Judd, Some aspects of the interactions among nucleation sites during saturated nucleate boiling, Int. J. Heat Mass Transfer 28 (12) (1985) 2331–2342.
[3] I. Golobič, H. Gjerkeš, Interactions between laser-activated nucleation sites in pool boiling, Int. J. Heat Mass Transfer 44 (2001) 143–153.

[4] S.H. Bhavnani, S.E. Balch, R.C. Jaeger, Control of incipience hysteresis effects in liquid cooled electronics heat sinks, J. Electron. Manufact. 9 (2) (1999) 179–190.
[5] C.S. Baldwin, S.H. Bhavnani, R.C. Jaeger, Towards optimizing enhanced surfaces for passive immersion cooled heat sinks, IEEE Trans. Compon. Packag. Technol. 23 (1) (2000) 70–79.
[6] S.M. You, T.W. Simon, A. Bar-Cohen, Reduced incipient superheat in boiling of fluids which hold dissolved gas content, ASME HTD, Phase Change Heat Transfer 159 (1991) 109–117.
[7] G.M. Chrysler, R.C. Chu, R.E. Simons, Jet impingment boiling of a dielectric coolant in narrow gaps, in: 1994 InterSociety Conference on Thermal Phenomena, Washington, DC, 4–7 May 1994, pp. 1–8.
[8] J.Y. Chang, S.M. You, Boiling heat transfer phenomenon from micro-porous and porous surfaces in saturated FC 72, Int. J. Heat Mass Transfer 40 (18) (1997) 4437–4447.
[9] H. Kubo, H. Takamatsu, H. Honda, Effect of size and number density of micro-reentrant cavities on boiling heat transfer from a silicon chip immersed in degassed and Gas-Dissolved FC-72, Enhanced Heat Transfer 6 (1999) 151–160.
[10] S. Moghaddam, M. Ohadi, J. Qi, Pool boiling of water and FC 72 on copper and graphite foams, CD-ROM Paper No. IPACK2003-35316, in: Proceeding of the ASME InterPACK 2003, Maui, Hawaii.
[11] M.S. El-Genk, J.L. Parker, Pool boiling in saturated and subcooled FC-72 dielectric fluid from a porous graphite surface, CD-ROM Paper No. IMECE2004-59905, in: Proceedings of the 2004 ASME International Mechanical Engineering Congress and Exposition, Anaheim, CA, USA, 2004.
[12] P.W. McFadden, P. Grassmann, The relation between bubble frequency and diameter during nucleate pool boiling, Int. J. Heat Mass Transfer 5 (1961) 169–173.
[13] H.J. Ivey, Relationships between bubble frequency, departure diameter and rise velocity in nucleate boiling, Int. J. Heat Mass Transfer 10 (1967) 1023–1040.
[14] R.L. Judd, K.S. Hwang, A comprehensive model for nucleate pool boiling heat transfer including microlayer evaporation, Trans. ASME, J. Heat Transfer 98 (4) (1976) 623–629.
[15] N. Nakayama, T. Daikoku, H. Kuwahara, T. Nakajima, Dynamic model of enhanced boiling heat transfer on porous surfaces, Part I and II, Trans. ASME, J. Heat Transfer 102 (1980) 445–456.
[16] G. Fournelle, S.H. Bhavnani, R.C. Jaeger, Optical study of enhanced heat transfer from a heat sink for microelectronics applications, Advances in Electronic Packaging '1999 26 (2) (1999) 1463–1469.
[17] S.H. Bhavnani, G. Fournelle, R.C. Jaeger, Immersion-cooled heat sinks for electronics: insight from high-speed photography, IEEE Trans. Compon. Packag. Technol. 24 (2) (2001) 166–176.
[18] C.C. Pascual, S.M. Jeter, S.I. Abdel-Khalik, Visualization of boiling bubble dynamics using a uniformly heated transparent surface, Technical Note, Int. J. Heat Mass Transfer, 45 (2002) 691–696.
[19] D.P. Rini, C. Ruey-Hung, L. Chow, Bubble behavior and heat transfer mechanism in FC 72 pool boiling, Exp. Heat Transfer 14 (2001) 27–44.
[20] C. Ramaswamy, Y. Joshi, W. Nakayama, W.B. Johnson, High-speed visualization of boiling from an enhanced structure, Int. J. Heat Mass Transfer 45 (2002) 4761–4771.
[21] L. Zhang, M. Shoji, Nucleation site interaction in pool boiling on the artificial surface, Int. J. Heat Mass Transfer 46 (2003) 513–522.
[22] N.D. Nimkar, S.H. Bhavnani, C.D. Ellis, R.C. Jaeger, Development of an anodically-bonded test surface to obtain fundamental liquid immersion thermal management data for electronic devices, Sensors Actuators A 113 (2004) 212–217.
[23] N.D. Nimkar, Benchmark one dimensional heat transfer data for an enhanced surface: optical study and analysis of boiling phenomenon, M.S. Thesis, Auburn University, AL, 2003.
[24] S.J. Kline, F.A. McKlintock, Describing uncertainties in single sample experiments, Mech. Eng. 75 (1953) 3–8.